第 32 卷第 3 期
2016 年 3 月

无 机 化 学 学 报
CHINESE JOURNAL OF INORGANIC CHEMISTRY

Vol.32 No.3
527-536

基于导电基底的多孔银耳状氧化镍的电化学行为

韩丹丹* 徐鹏程 谭 奥 于江微 张立平 张 涛
(吉林化工学院化学与制药工程学院,吉林 132022)

摘要: 采用化学沉淀法,在导电基底上原位生长多孔状氧化镍。采用 X 射线衍射(XRD)、扫描电镜(SEM)和透射电子显微镜(TEM)对其结构和形貌进行了表征。采用循环伏安、恒流充放电技术和交流阻抗对其电化学性能进行了测试。结果表明,由于泡沫镍导电基底增强了电极的导电性, 充分利用各组成单元的多孔特性, 在电流密度为 0.5 $A\cdot g^{-1}$ 时, 电极的比容量达到 3.5 $F\cdot cm^{-2}$ (705 $F\cdot g^{-1}$),同时电极具有较好的倍率特性(电容保持率 68.1%)和稳定的长循环寿命(3 000 次循环后电极比容量增加 17.6%)。

关键词: 氧化镍; 超级电容器; 化学沉淀法; 导电基底
中图分类号: O646 **文献标识码**: A **文章编号**: 1001-4861(2016)03-0527-10
DOI: 10.11862/CJIC.2016.052

Porous Tremella-like NiO on Conductive Substrates with High Electrochemical Performance

HAN Dan-Dan* XU Peng-Cheng TAN Ao YU Jiang-Wei ZHANG Li-Ping ZHANG Tao
(*College of Chemistry and Pharmaceutical Engineering, Jilin Institute of Chemical Technology, Jilin, Jilin* 132022, *China*)

Abstract: Porous tremella-like NiO on conductive substrates have been fabricated by a facile chemical bath deposition approach and further investigated as the binder-free electrode for high-performance supercapacitors. The microstructure and morphologies of the resulting materials were characterized by XRD, SEM, TEM, and electrochemical measurements. Owing to the superior electrical conductivity, the porous structure of the NiO microspheres combinated the advantages of each subunit can deliver a high areal capacitance of 3.5 $F\cdot cm^{-2}$ and a corresponding specific capacitance of 705 $F\cdot g^{-1}$ at a current density of 0.5 $A\cdot g^{-1}$, as well as a good rate capability (68.1% capacitance retention from 0.5 $A\cdot g^{-1}$ to 8 $A\cdot g^{-1}$), and excellent cycling stability (17.6% capacitance increasing after 3000th cycling at high current density 12 $A\cdot g^{-1}$).

Keywords: nickel oxide; supercapacitor; chemical bath deposition; conductive substrate

0 Introduction

As energy storage devices, the high power and energy outputs, long lifetime, and short charging time are urgently needed to meet the increasing demand for energy and power in our daily life[1-3]. Supercapacitors hold great potential as energy storage devices with some excellent properties such as high power density, long cycle life, fast charge time, and safe operation mode[4-6]. However, as compared to rechargeable lithium batteries, supercapacitors suffer from relatively lower energy density[7]. In recent years, great research

收稿日期:2015-08-22。收修改稿日期:2016-01-09。
国家自然科学基金项目(No.21401073)吉林省科技厅青年基金项目(No.20140520097JH)、博士科研启动基金(No.2014161)、吉林化工学院科技项目(No.2014064)资助。
*通信联系人。E-mail:luckhan2006@163.com

progress has been accomplished for the improvement of supercapacitor performance by the fabrication of electrodematerials with unique special structure[8-12]. It is well know that nickel oxide (NiO) has been intensively studied as supercapacitors for its high theoretical specific capacitance of 2 584 $F \cdot g^{-1}$ [13-14]. Thus, it can display a wonderful electrochemical performance. For example, Muralidharan and co-workers successfully obtained NiO nanoflakes with largely enhanced electrochemical performance (401 $F \cdot g^{-1}$ at a current density of 0.5 $mA \cdot cm^{-2}$ and 92% of specific capacitance could be retained after 500 cycles) through a simple microwave method [15]. Though NiO shows a remarkable electrochemical performance, the experimental values of specific capacitance are still much lower than its theoretical values and not satisfactory for practical application. It is partially due to the existent of the nonconductive polymer binder, which will lead to an extra contact resistance and dead surface, thus hindering the diffusion of KOH electrolyte. Therefore, it is desirable to grow electrode materials on current collector directly and be used as a binder-free electrode [16-18]. Thus, Co_3O_4 nanoflowers on Ni foam have been prepared and the capacity retention of 78.2% after 1 000th cycling at a current density of 3 $A \cdot g^{-1}$[19].

Since the lightweight and flexibility of the electrodes is closely related to the electrochemical activity and structural stability of the material, exploring scalable and facile synthetic process for the preparation of unique morphologies of NiO is great importance. For example, as a dry route to NiO nanoparticles, conventional gas phase-based synthetic strategies such as flame synthesis have been developed [20-21]. Alternatively, wet chemical route has been proposed as a cost-effective and facile procedure for the controllable synthesis of NiO on the conductive substrates. Commonly, layered nickel hydroxide ($Ni(OH)_2$) with various morphologies can be conveniently synthesized in solutions of Ni(Ⅱ) by a chemical precipitation method, while NiO can be conveniently prepared by copy the morphology of $Ni(OH)_2$. Consequently, as a result of the monoclinic or brucite crystallographical structures of $Ni(OH)_2$, the obtained NiO nanomaterials are mostly in 2D forms of nanoplate or nanoflake. It is well known that 1D nanowires or 2D nanoflakes can act as the building block to construct complex and multifunctional architectures [22-24]. Therefore, In order to get a better electrochemical performance for a pseudocapacitor, it is highly desirable to engineer electrodes with the combination of the advantages of each subunit [25-29]. Thus, the unique tremella-like NiO consisting of nanosheets with open space between neighboring nanostructures facilitates the diffusion of electrolyte into the inner region of the electrode, particularly helpful for reducing internal resistance and improving high-power performance[30].

From a practical point of view, developing a binder-free electrode with a mild and cost-effective process without using high pressure and temperature remains an urgent challenge. In line with the aim of a green and scalable synthesis, we report a chemical bath deposition (CBD) process capable of the large-scale synthesis of NiO with a tremella-like structure growth on variety of substrates including transparent conducting glass, and nickel foam. The superior supercapacitor performance of the electrodes based on NiO grown on nickel foam will be demonstrated. Benefiting from favorable porous structure as well as the rational design of a binder-free electrode, the electrode exhibits a much higher capacitance (705 $F \cdot g^{-1}$ at a current density of 0.5 $A \cdot g^{-1}$) and excellent cycling ability after 3 000th cycling with different current. It can be concluded that the facile design of a binder-free NiO nanostructure would be particularly suited to the high-performance electrodes for supercapacitors.

1 Experimental

1.1 Preparation of the products

All the chemicals are of analytical grade and were used without further purification. Self-supported tremella-like NiO were prepared by a facile chemical solution process. The solution was prepared by dissolving 0.79 g $NiSO_4$, 0.20 g $(NH_4)_2SO_4$, and 4.5 mL

of NH_4OH in 10 mL of distilled water to form a homogeneous solution with magnetic stirring for 5 min. Then this resulting solution was transferred into the sealed flask. Various substrates such as FTO glass (10 mm×30 mm in size), and nickel foam (10 mm× 10 mm×1.1 mm, 110 PPI, 320 $g \cdot m^{-2}$, Changsha Lyrun Material Co., Ltd. China) were immersed into the reaction solution for 6 h at 90 ℃ to allow growth of nanostructure and then cooled to room temperature. The samples were collected and rinsed with distilled water several times. Finally, the samples were annealed at 300 ℃ in air for 1.5 h.

1.2 Characterizations

The morphologies of the samples were inspected on a scanning electron microscope (SEM, JSM-6480A, Japan Electronics). X-ray diffraction (XRD) measurement was examined on a Rigaku D/max TTR-III diffractometer using Cu $K\alpha$ radiation (λ=0.154 05 nm). Transmission electron microscopy (TEM) micrographs were performed on a FEI Tecnai G^2 20 S-TWIN transmission electron microscope with a field emission gun operating at 200 kV.

1.3 Electrochemical measurements

The self-supported tremella-like NiO were directly used as the working electrode. The electrochemical tests were conducted with a CHI 660E electrochemical workstation in an aqueous KOH electrolyte (2.0 $mol \cdot L^{-1}$) with a three-electrode cell where Pt foil serves as the counter electrode and a saturated calomel electrode (SCE) were used as the counter and reference electrodes. The loaded weight of NiO nanoflower was controlled to be approximately 5 $mg \cdot cm^{-2}$. The EIS measurements were carried out in the frequency range from 100 kHz to 0.05 Hz at open circuit potential with an ac perturbation of 5 mV.

2 Results and discussion

2.1 Material characterization

To study the crystallinity and crystal phases of the as-obtained product, the prepared tremella-like NiO were analyzed by X-ray diffraction. Fig.1 shows the XRD pattern of the NiO/Ni electrode, together with the porous NiO powder scratched down from Ni foam for comparison. For the NiO/Ni electrode, except for peaks originating from the nickel substrate, the peaks at 37.2°, 43.3°, 62.8°, 73.4°, and 79.4° could be indexed as (111), (200), (220), (311), and (222) crystal planes of the NiO phase (JCPDS No. 47-1049), respectively. No peaks of other phases are observed, these indicate that high-purity NiO are obtained during the synthetic process.

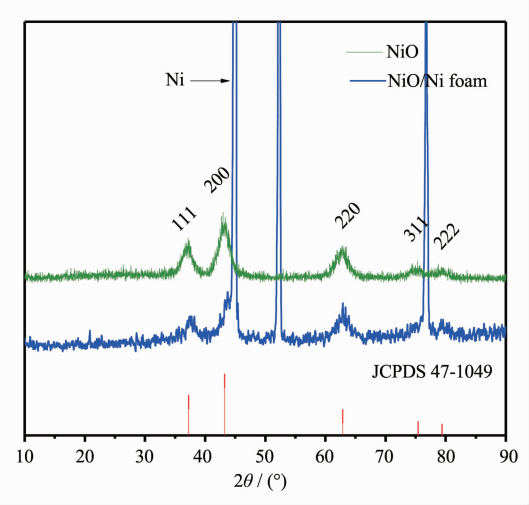

Fig.1　XRD patterns of tremella-like NiO scratched down from Ni foam and NiO/Ni sample as indicated by different colours

The morphologies of the tremella-like NiO on nickel foam was conducted using SEM. Fig.2a shows a low-resolution image of the Ni foam without any active materials, which has a smooth 3D structure before the tremella-like NiO growth. Fig.2b ~d show the SEM images of the tremella-like NiO spheres on Ni foam at different magnifications. It can be observed that the nickel foam is uniformly covered by the

NiO sphere on a large scale (Fig.2b). As observed from the high magnification SEM image, the porous NiO spheres self assembled from nanoflakes display tremella-like nanostructure with diameters of 10 ~15 μm (Fig.2c and d). Though some micro-tremella are overlapped each other, the highly porous structure can still provide plenty of channels for the transportation of KOH electrolyte into the inner area of the NiO electrode material, which is great importance to effective utilization of the NiO electro-active materials.

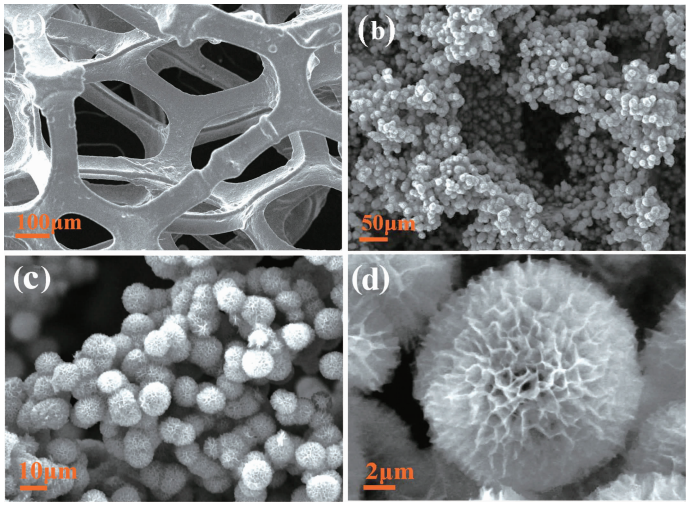

Fig.2 SEM images of a Ni foam (a), tremella-like NiO grown on Ni foam (b,c); (d) Enlarged view of the porous spheres showing the tremella-like morphology

The photographs of the Ni foam (left), precursor as-prepared (middle) and tremella-like NiO on Ni foam (right) are shown in Fig.3a. The Ni foam turns to a green color after reaction, suggesting the formation of nickel hydroxide on the Ni foam. When annealed at 300 ℃ for 1.5 h, the green Ni foam turns to a black color, the tremella-like NiO was formed. TEM studies provide further insight into the unique porous NiO spheres. Fig.3b shows a low-resolution TEM image of the NiO scratched down from the Ni foam substrate. Several pieces of random nanosheets clearly can be found. The curl edge of the flake in Fig.3b further verifies that the tremella-like NiO are constructed by flexible ultrathin nanosheet building blocks. Interestingly, as depicted in the higher magnification TEM image (Fig.3c and d), numerous pores ranging from 2 to 5 nm are observed, which are generated by the rapid release of water molecules during the

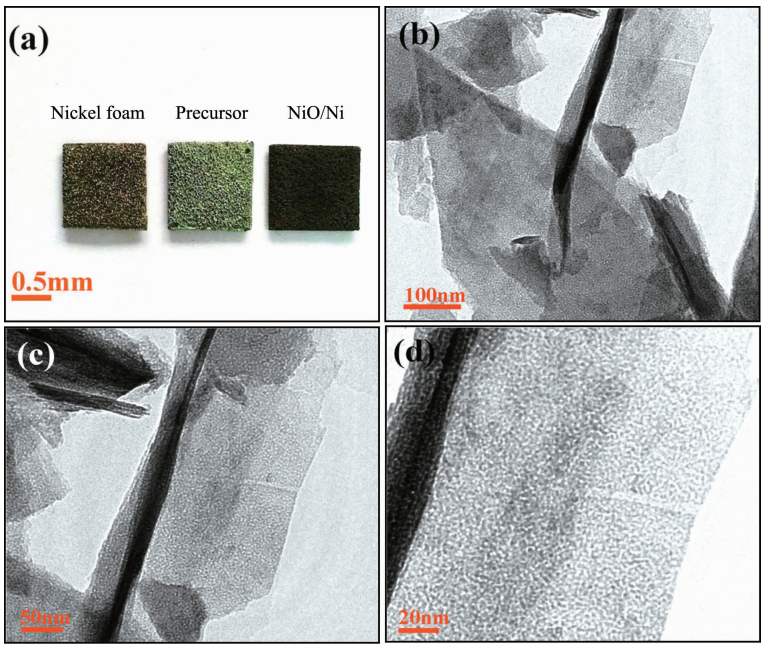

Fig.3 (a) Photographs of Ni foam (left), precursor as prepared (middle) and NiO (right); Low (b) and high (c,d) magnification TEM images of an individual NiO nanosheet

conversion of $Ni(OH)_2$ into NiO [31]. Moreover, the existence of mesopores could provide more sites for the KOH electrolyte ions and facilitate fast ion diffusion during the charge-discharge process. Since the fast and efficient synthetic method wide application of nickel foam deposition for metal hydroxides and oxides, which can be applied in and extended to the fabrication of other nanostructure on the slide surface, such as FTO (Fig.4a and b). Herein, the tremella-like NiO were also prepared via the same methodology. Differently, the density of NiO spheres increases and thereby the open space between neighboring spheres decreases. Moreover, the morphology and diameters of the NiO active materials can be easily varied by choosing different reagent. If nickel nitrate is the nickel source, the tremella-like NiO can not be seen. Inversely, the $Ni(OH)_2$ nanoparticals can be chemically assembled on the Ni foam to form winding coil-like arrays with the reaction time prolong to 5 h, which change into the unique nanostructure after annealing at 300 ℃ (Fig.4c and d).

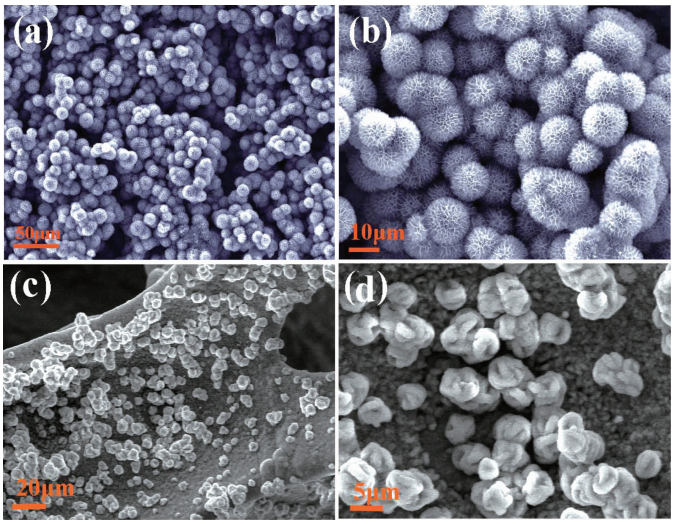

Fig.4　(a, b) SEM images of the NiO nanoflower grown on FTO substrate; (c,d) SEM images of the winding coil-like NiO using $Ni(NO_3)_2$ as nickel source by the reaction time 5 h

The growth mechanism of tremella-like NiO is proposed as below. The freestanding NiO nanostructure comes from basic nickel hydroxide $Ni(OH)_2$ nanostructure after heat-treatment. The tremella-like NiO consists of numerous interconnected nanocrystallites and possesses a large quantity of mesopores, which is ascribed to the successive release and loss of CO_2 and H_2O during the thermal decomposition of $Ni(OH)_2$ precursor (Fig.5). The growth of $Ni(OH)_2$ is a result of their layered brucite crystal structure of the CdI_2 type, which has a weak interaction between layers and strong binding within the layered planes [32]. Neighboring layers are bound together by weak Van der Waal forces, and thus the (001) planes are stable ones with the lowest surface energy. Taken together, the presented synthesis method is very robust and may lead to growth of other oxide or hydroxide arrays on various conductive substrates. This nanostructure shows some interesting characteristics such as high porosity and direct growth on conductive substrates, which make them potential building blocks for electrochemical energy storage and catalysis.

To explore the potential application of the as-synthesized tremella-like NiO, the sample was fabricated as supercapacitor electrodes and characterized by CV, EIS, and galvanostatic charge/discharge measurements. Fig.6a presents CV curves of the unique tremella-like NiO electrode at various scan rates ranged from 5 to 50 $mV \cdot s^{-1}$ in the potential window of 0 to 0.45 V (vs SCE). The electrode are subjected to one time stabilization/activation by

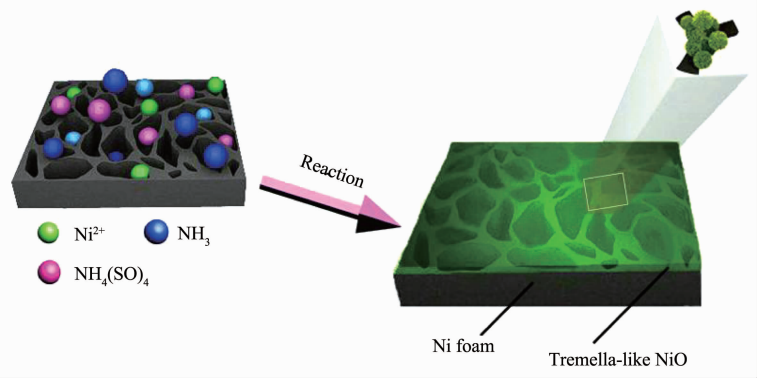

Fig.5 Schematic mechanism for the direct-growth process of tremella-like NiO on the Ni foam

repeated CV cycles (25 numbers) at sweep rate of 10 mV·s^{-1} in the similar potential range, before performing the CV experiments for accessing the electrochemical performance. Notably, electrochemical response currents of the CV curves on the positive sweeps are nearly mirror-image symmetric to their corresponding counterparts on the negative sweeps with respect to the zero-current line. Also, as the scan rate increases, the current subsequently increases while the CV shape changes little and rapid current response on voltage reversal occurs at each end potential, which indicates good electrochemical capacitive nature for the unique porous electrode. A distinct pair of current peaks can be identified during the cathodic and anodic sweeps, whose intensity increases with the change of the scan rate. It can be attributed to the following reversible redox reaction:

$$NiO+zOH^- \rightarrow zNiOOH+(1-z)NiO+ze^- \quad (1)$$

A pair of redox peaks is located at around 0.193 and 0.302 V with the scan rate of 5 mV·s^{-1}. After the 25-fold increase in the sweep rate from 5 to 50 mV·s^{-1}, the position of the cathodic peak shifts slightly from 0.193 to 0.159 V. This observation suggests a relatively low resistance of the electrode because of the good contact between the electroactive NiO nanosheets and the conductive Ni foam substrate. The specific capacitance of the electrode can be calculated from the CV curves according to the following equation[33-35]:

$$C_s = (1/vw(\Delta v)) \int_{v_a}^{v_c} i dv \quad (2)$$

where Δv (V) is the applied potential window (v_a to v_c) and w (g) is the weight of the active material. At potential scan rates of 30 mV·s^{-1}, the specific capacitance values for tremella-like NiO spheres calculated before and after charge/discharge cycles is found to be 820.7 F·g^{-1} and 865.9 F·g^{-1}, respectively (Fig.6b). Clear enhancement in the specific capacitance value is observed which is possibly due to the structural activation and pore opening of the sample during the charge/discharge process. It is known that the characteristics of redox reactions are strongly dependent on the shape and dimensionality of the electrode material at the nanoscale level[36]. Higher specific area and suitable porosity for easy insertion/de-insertion of ions into/from the electrode matrix mostly contribute to the number, efciency and ease of redox reactions. The tremella-like NiO spheres consist of uniform multilayer nanosheet as compared to the lowly porous bulk spheres sample which have higher efficiency specific area and promote higher number of redox reactions resulting in higher specific capacitance.

The typical charge and discharge curves of the two electrodes at different current densities within the potential window of 0~0.4 V are shown in Fig.6c. The areal and specific capacitance for the NiO electrodes can be calculated on the basis of the charge and discharge curves, and the results are presented in Fig. 6d. The specific capacitance values have been calculated from the applied current density (i), mass of the NiO sample (m), discharge time (Δt), and

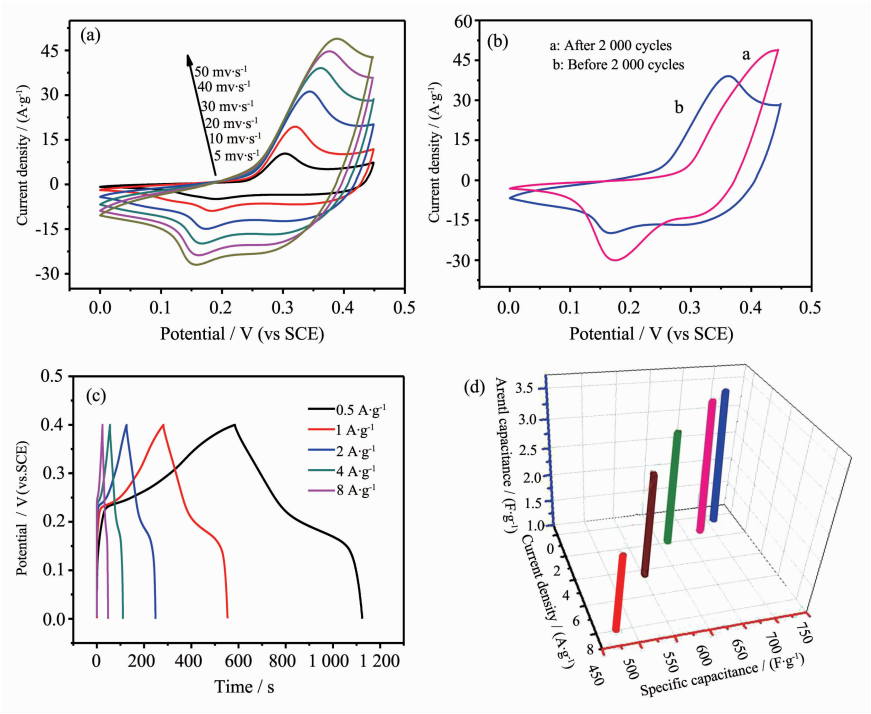

Fig.6　(a) Cyclic voltammetry curves of tremella-like NiO at scan rate of 5, 10, 20 and 50 mV·s^{-1}, (b) comparison of cyclic voltammograms at a scan rate of 30 mV·s^{-1} before and after 2 000 charge-discharge cycles, (c) the discharge curves of tremella-like NiO between voltage limits of 0 to 0.4 V at rates varied from 0.5 A·g^{-1} to 8 A·g^{-1} and (d) specific capacitance and areal capacitance vs current density

operating potential (ΔV) using the equation[37-39]:

$$C_s = i/m(\Delta V/\Delta t) \quad (3)$$

The specific capacitances are calculated by subtracting the discharge time of bare nickel foam at the same current density. The tremella-like NiO electrodes show specific capacitance values of 705, 680, 615, 560, 480 F·g^{-1} at different current densities of 0.5, 1, 2, 4 and 8 A·g^{-1}, respectively. These values are much higher than those of the single $NiCo_2O_4$ electrodes (470 F·g^{-1} at 5 A·g^{-1}) and other metal composite oxides films such as Co_3O_4@$NiCo_2O_4$ (0.89 F·cm^{-2} at 1.6 mA·cm^{-2})[40-41].

Electrochemical impedance spectroscopy (EIS) has been applied to investigate the details of the electrochemical characteristics of the NiO-based electrode before and after the long-term cycling test. The Nyquist plots extracted from the EIS of NiO electrode before and after 1 000th, 3 000th cycling at an applied potential of 5 mV are shown in Fig.7. A well-fitted equivalent circuit in the inset of Fig.7 shows the components of the whole impedance. The elements in the equivalent circuit include the solution resistance (R_s), the double-layer capacitance (C_{dl}), the charge-transfer resistance (R_{ct}), the Warburg diffusion element (W), and the pseudocapacitance element (C_{ps}). It can be observed that the value of R_s, obtained by the intercept on the real axis in the high-frequency range, has no remarkable change after 3 000th cycling, which suggests the stability in the electron conductivity of the NiO/Ni electrode. In addition, the

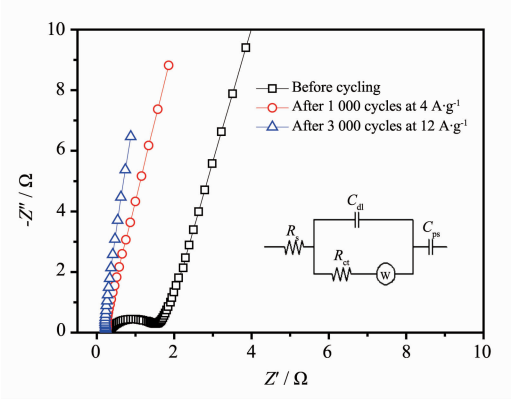

Fig.7　yquist plots of tremella-like NiO sample before and after 3 000 charge-discharge cycles

slope at the low frequency region is still close to 90° after 1 000th and 3000th cycling, and there is near absence of semicircles at the high frequency region. This indicates that the capacitive behavior of tremella-like NiO is almost identical and suggests no appreciable change in structural and electrochemical characteristics during high rate cycling.

The plots of frequency dependent real (C') and imaginary (C'') components of capacitance before and after the long-term cycling are shown in Fig.8. At low frequency, electrolyte ions penetrate deep inside the pores of the carbon material accessing more electrode surface thereby contributing to the high capacitance value. At higher frequencies electrolyte ions can only have access to the surface of materials whereas the inner pores are not accessed giving rise to a sharp decrease in the capacitance. The sharp peak in the graph of the frequency dependent imaginary component of capacitance (C'') shows a maximum capacitance (C'') at a frequency f_0 which corresponds to the relaxation time as $\tau_0=1/f_0$ which is ~2.6 s (Fig.8a). This value is much lower than that of the electrode before 3 000th cycling (~19.2 s). The low relaxation time (~2.6 s) also indicates the maximum accessibility of the outer surface of the NiO electrode material to the electrolyte ions.

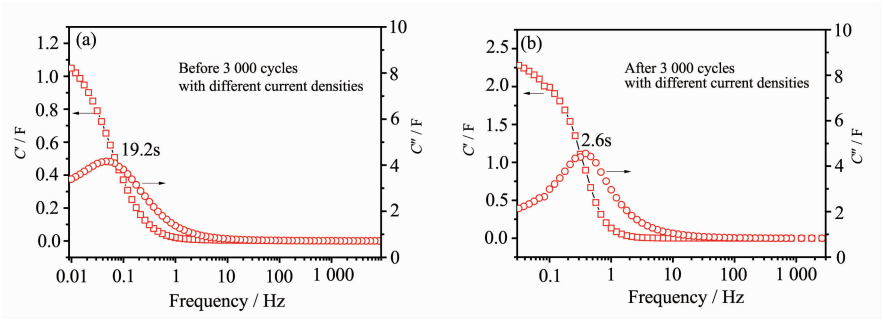

Fig.8 Evolution of the real and imaginary part (C' and C'') of the stack capacitance before and after long cycles

As a critical parameter to determine the energy storage performance for practical applications, the long-term cycling stability of our asymmetric sueprcapacitor is tested and shown in Fig.9a. The Ni foam-supported tremella-like NiO electrode is first cycled with a current density of 4 A·g^{-1}, and then the current density is increased to 8 A·g^{-1} and 12 A·g^{-1}, successively. Even after sudden change of the current delivery, the free-standing tremella-like NiO electrode also exhibits excellent stability at each current density. When a discharge current density of 4 A·g^{-1} is applied, the specific capacitance reaches a value of 560 F·g^{-1} in the initial cycle. After 1 000 cycles, the electrode displays an excellent long cycle life with 7% increasing of its initial specific capacitance, demonstrating superior long-term electrochemical stability. Even at a high charging/discharging current density of 12 A·g^{-1}, the specific capacitance can still

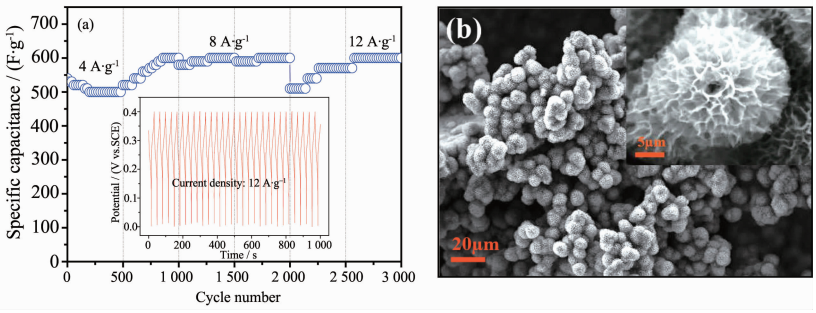

Fig.9 (a) Cycling performance of porous tremella-like NiO on nickel foam at different current density, (b) SEM image of tremella-like NiO grown on Ni foam after 3 000 cycles at different current density

reach 510 F·g^{-1} in the first cycle, under this condition. After further 1 000 times of continuous cycling at 12 A·g^{-1}, the unique electrode increases 17.6% of the specific capacitance at the 3 000th cycling (600 F·g^{-1}). It is known that retaining the structure integrity is a key factor to ensure the good cyclability of the material [42-43]. The SEM image (Fig. 9b) of the tremella-like NiO electrode is also shown after 3 000 cycles. It can be observed that unique 3D structure electrode still keeps its primary structure. Such data further highlights the capability of the unique free-standing tremella-like NiO electrode to meet the requirements of both long cycling performance and good rate capability, which are important merits for the practical energy storage devices.

3 Conclusions

We have demonstrated the fast and convenient method for the growth of tremella-like NiO by direct deposition on different conductive substrates toward the formation of self-supported electrode. Owing to the porous nanosheets and the unique multilayers structure of the NiO/Ni active material, excellent cycling stability, 7% specific capacitance increasing at current density 4 A·g^{-1} for 1 000th cycling and 17.6% specific capacitance increasing for a 3-time current density rise, is achieved. Additionally, the well-contaction of the active tremella-like NiO with Ni substrate enables fast electron-transfer leading to the low internal resistance, which is especially important for the improvement of the electrochemical performance of ECs. So the present low-cost NiO/Ni strucure can serve as a promising electrode material for high performance supercapacitors.

References:

[1] Conway B E. *Electrochemical Supercapacitors*: *Scientific Fundamentals and Technological Applications*. New York: Plenum Press, **1999**.

[2] Bi R R, Wu X L, Cao F F, et al. *J. Phys. Chem. C*, **2010**, **114**:2448-2451

[3] Xu C, Xu B, Gu Y, et al. *Energy Environ. Sci*., **2013**,**6**: 1388-1414

[4] Simon P, Gogotsi Y. *Nat. Mater*., **2008**,**7**:845-854

[5] Miller J R, Simon P. *Science*, **2008**,**321**:651-652

[6] Liu J L, Zhang L L, Wu H B, et al. *Energy Environ. Sci.*, **2014**,**7**:3709-3719

[7] Wang H W, Hu Z A, Chang Y Q, et al. *J. Mater. Chem*., **2011**,**21**:10504-10511

[8] Gao Y Y, Chen S L, Cao D X, et al. *J. Power Sources*, **2010**, **195**:1757-1760

[9] Yan X Y, Tong X L, Wang J, et al. *J. Alloys Compd.*, **2014**, **593**:184-189

[10]Kim J Y, Lee S H, Yan Y, et al. *RSC Adv*., **2012**,**2**:8281-8285

[11]Du D M, Hu Z H, Deng Y H, et al. *J. Alloys Compd.*, **2014**, **589**:82-87

[12]Xia X H, Tu J P, Wang X L, et al. *J. Mater. Chem*., **2011**, **21**:671-679

[13]Liu M C, Kong L B, Lu C, et al. *J. Mater. Chem. A*, **2013**, **19**:1380-1387

[14]Ding S J, Zhu T, Chen J S, et al. *J. Mater Chem*., **2011**,**21**: 6602-6606

[15]Vijayakumar S, Nagamuthu S, Muralidharan G, et al. *ACS Appl. Mater. Interfaces*, **2013**,**5**:2188-2196

[16]Deng F Z, Yu L, Cheng G, et al. *J. Power Sources*, **2014**,**251**:202-207

[17]Liu X Y, Zhang Y Q, Xia X H, et al. *J. Power Sources*, **2013**,**239**:157-163

[18]Chen H C, Jiang J J, Zhang L, et al. *J. Power Sources*, **2014**,**248**:28-36

[19]Qing X X, Liu S Q, Huang K L, et al. *Electrochim. Acta*, **2011**,**56**:4985-4991

[20]Tricoli A, Righettoni M, Teleki A, et al. *Angew. Chem. Int. Ed.*, **2010**,**49**:7632-7659

[21]Azurdia J A, Marchal J, Shea P, et al. *Chem. Mater*., **2006**, **18**:731-739

[22]Nguyen V H, Shim J J. *J. Power Sources*, **2015**,**273**:110-117

[23]Cai D P, Wang D D, Liu B, et al. *ACS Appl. Mater. Interfaces*, **2014**,**6**:5050-5055

[24]Wijeratne K, Bandara J. *Electrochim. Acta*, **2014**,**148**:302-304

[25]Mai L Q, Yang F, Zhao Y L, et al. *Nat. Commun.*, **2011**,**2**: 381-385

[26]Zhou W, Cheng C, Liu J, et al. *Adv. Funct. Mater*., **2011**, **21**:2439-2445

[27]Cui L F, Yang Y, Hsu C M, et al. *Nano Lett*., **2009**,**9**:3370-3374

[28]Xia X, Tu J, Zhang Y, et al. *ACS Nano*, **2012**,**6**:5531-5538

[29]Mai L Q, Tian X C, Xu X, et al. *Chem. Rev*., **2014**,**114**:11828-11862

[30]Gong X F, Cheng J P, Liu F, et al. *J. Power Sources*, **2014**,**267**:610-616

[31]Wu H, Xu M, Wu H, et al. *J. Mater. Chem*., **2012**,**22**:19821-19825

[32]Xia X H, Tu J P, Zhang Y Q, et al. *Chem. Mater*., **2012**,**24**:3793-3799

[33]Srinivasan V, Weidner J W. *J. Power Sources*, **2002**,108:15-20

[34]Zhao X, Wang A, Yan J, et al. *Chem. Mater.*, **2010**,**22**:5463-5473

[35]Kim C H, Kim B H. *J. Power Sources*, **2015**,**274**:512-520

[36]Ghodbane O, Pascal J L. *ACS Appl. Mater. Interfaces*, **2009**, **1**:1130-1139

[37]Yuan C Z, Hou L R, Feng Y L, et al. *Electrochim. Acta*, **2013**,**88**:507-512

[38]Chen Y Z, Liu Y N, Yan W. *J. Mater. Chem. A*, **2014**,**2**:5903-5909

[39]Li Z, Xu Z W, Tan X H, et al. *Energy Environ. Sci*., **2013**,**6**:871-878

[40]Chen H C, Jiang J J, Zhang L, et al. *J. Power Sources*, **2014**,**248**:28-36

[41]Li Y H, Zhang Y F, Li Y J, et al. *Electrochim. Acta*, **2014**,**145**:177-184

[42]Zhang F, Yuan C Z, Lu X J, et al. *J. Power Sources*, **2012**,**203**:250-256

[43]Li Y G, Tan B, Wu Y Y. *Nano Lett.*, **2008**,**8**:265-270